International Journal of Multidisciplinary Research and Growth Evaluation.

CFD Application Simulation & Research on the Influence of Maneuver Angle on Aerodynamic Forces Used on Cars

Nguyen Tri Nguyen [1], Le Thi Minh Nghia [2], Bui Quoc Khoa [3*]
[1] Nong Lam University, HCMC, Vietnam
[2] Institute for Computational Science and Technology, Vietnam
[3] Van Lang University, Vietnam

* Corresponding Author: **Bui Quoc Khoa**

Article Info

ISSN (online): 2582-7138
Volume: 06
Issue: 01
January-February 2025
Received: 05-11-2024
Accepted: 09-12-2024
Page No: 292-298

Abstract
Nowadays, the automobile industry is increasingly developing, along with the requirements of reducing fuel consumption, the design of cars with good aerodynamic shape is of interest to many countries in the world. Therefore, reducing aerodynamic drag is one of the issues that car designers put first. The method of simulating fluid flow through the car uses the finite volume method for unstructured mesh, using Fluent software based on the Reynolds Navier - Stokes average equation and the standard k - ε turbulence model. The accuracy of the problem depends on the number of grid points and the computer resources. The problem is solved by the sequential solution method. The simulation results are shown in intuitive graphics, which are the pressure and velocity distribution fields.

DOI: https://doi.org/10.54660/.IJMRGE.2025.6.1.292-298

Keywords: CFD simulation, Computational Fluid Dynamic, maneuver angle car, Turbulent air flow, air movement through the car

Introduction

Nowadays, with the strong development of the automobile industry, the number of cars in circulation in the world is increasing, so the use of fuel in the world is increasing, making the amount of oil in nature increasingly depleted. Therefore, this is also a problem for car designers, producing cars with the most economical fuel consumption. (Lamballais E., Sylvestrini S.H., 2002) [1, 14, 18].

There are many measures to reduce fuel consumption in cars such as designing engines with low fuel consumption, engines using different energy sources and designing cars with suitable shapes to have the smallest drag coefficient (C_d). (Pham M.V., Plourde F. and Doan Kim S., 2003) [2, 3, 45].

Using numerical methods in finding solutions for engineering problems has been used more widely and more accurately. Among those methods, the most prominent are methods such as: Finite Element Method, Finite Difference Method, Boundary Element Method. Especially for problems related to hydrodynamics, people use the Finite Volume Method.

In this paper, we introduce some results of calculating the change in the drag coefficient in the case of changing the car's maneuvering angle using FLUENT software. These results will be used to evaluate the established integral model.

2. Simulation method

2.1. Turbulence model k – ε

The standard model uses the following two equations for and ε :

$$\frac{\partial(\rho k)}{\partial t} = div(\rho k U) = div\left(\frac{\mu_t}{\sigma_k} gradk\right) + G_k - \rho\varepsilon$$

$$\frac{\partial(\rho\varepsilon)}{\partial t} = div.(\rho\varepsilon U) = div.\left(\frac{\mu_t}{\sigma_\varepsilon} grad.\varepsilon\right) + C_{1\varepsilon}\frac{\varepsilon}{k}G_k - C_{2\varepsilon}\rho\frac{\varepsilon^2}{k}$$

With: G_k is a quantity characterizing the turbulence dynamics (for every type of turbulence model this characteristic will be different), $C_1\varepsilon$, $C_2\varepsilon$: adjustable constants,: $\sigma_k, \sigma_\varepsilon$ are Prandtl coefficients for k and ε , respectively.

2.2. Computational model

The car type selected for the calculation is Mercedes-Benz C180K CLASSIC, with parameters as in Table 1

Table 1: *Mercedes-Benz C180K CLASSIC car parameters*

No.	Parameter	Value
01	Length basic (m)	2,715
02	Length (m)	4,652
03	Width (m)	1,728
04	High (m)	1,426
05	Distance from front axle to front of vehicle (m)	0,755
06	Distance from rear axle to rear of vehicle (m)	1,056
07	Wind resistance coefficient C_d	0,26
08	Total weight (kg)	1,965

The car moves on the road, so the car will move through the air stream. The air has a viscosity coefficient μ= 1.789.10^{-5} kg/m.s, and a density of ρ=1.225 kg/m^3. The car moves at a speed of 40 m/s, corresponding to a Reynolds number of 4.10^6. The calculation space has dimensions selected as shown in **Figure 1**.

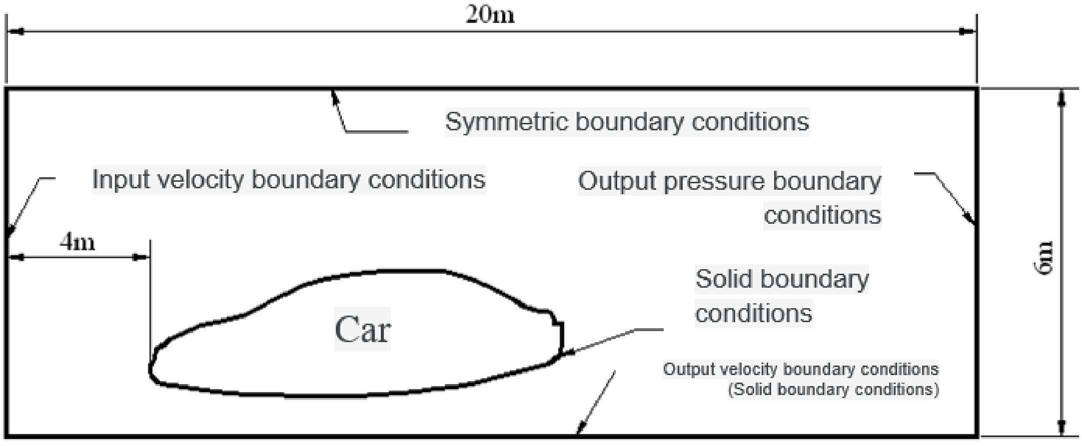

Fig 1: *Computational space and boundary conditions*

2.3. Meshing and boundary conditions

Mesh division: The density of the mesh has a great influence on the calculation results. In the area near the solid wall, the fluid changes greatly, so the mesh density here needs to be divided more finely to clearly show the change of the flow. The finer the mesh, the more clearly it shows the change of the flow and reduces the calculation error.

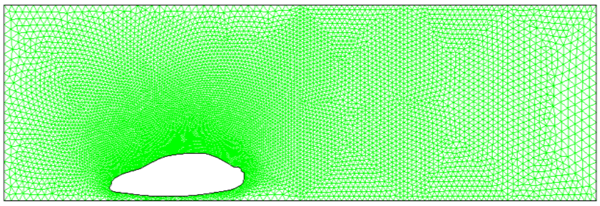

Fig 2: Spatial discrete model computed by Gambit with 17540 points

Boundary conditions: The boundary conditions of the computational domain are determined as shown in **Figure 1**, the values assigned to these boundary conditions are shown in **Tables 2 & 3**.

Table 2: Input velocity boundary conditions

Velocity (m/s)	$\vec{r}$	T (K)	I (%)	L (m)
40	(1,0,0)	303	5	0,05

Table 3: Outlet pressure boundary conditions

P (Pa)	T (K)	I (%)	L (m)
$9{,}81.10^4$	303	5	0,05

In which: I is the turbulence intensity, L is the characteristic turbulence length, temperature and pressure are selected according to actual external conditions.

3. Result

In this section, the author studies how changes in the front maneuver angle and rear maneuver angle affect aerodynamic properties? The choice of the computational space and boundary conditions is the same as above. The author will simulate a car running at a speed of 40 m/s. Consider a car with a front maneuver angle (α) and a rear maneuver angle (β) as shown in Figure 3. (Lamballais E., Sylvestrini S.H., 2002) [5, 62, 76].

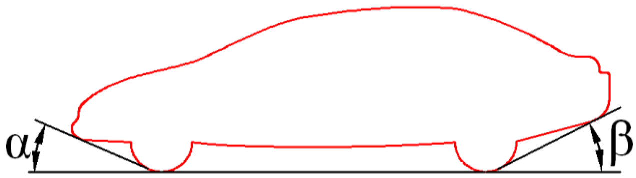

Fig 3: Car shape with front and rear maneuverability angles

3.1. Effect of forward maneuver angle (α)

In this section, we consider the effect of aerodynamic forces acting on the car when the front maneuver angle changes, the rear maneuver angle $\beta = 27^0$.

The simulation results are as follows:

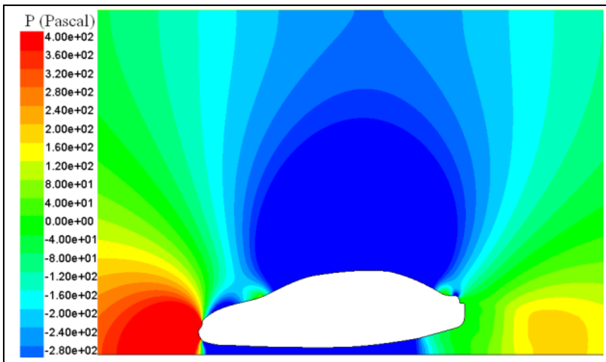

Fig 4: Pressure distribution on the calculation domain when $\alpha = 18^0$

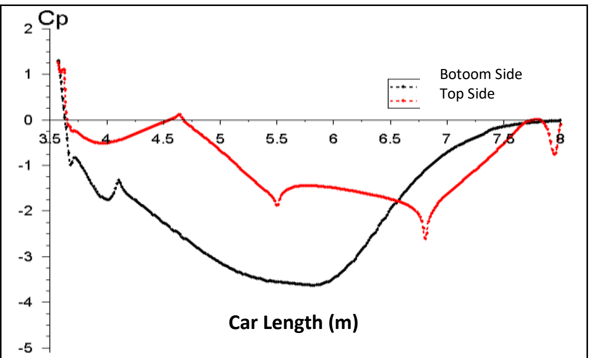

Fig 5: Distribution of pressure distribution coefficient on car when $\alpha = 18^0$

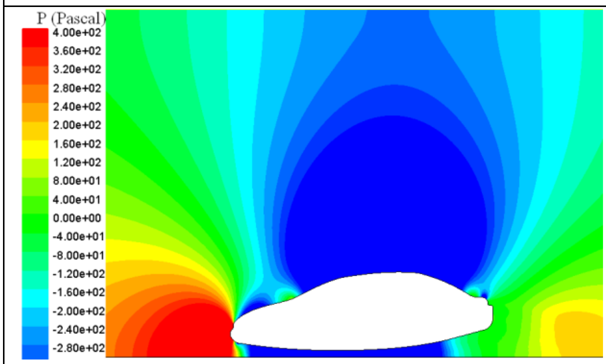

Fig 6: Pressure distribution on the calculation domain when $\alpha = 20^0$

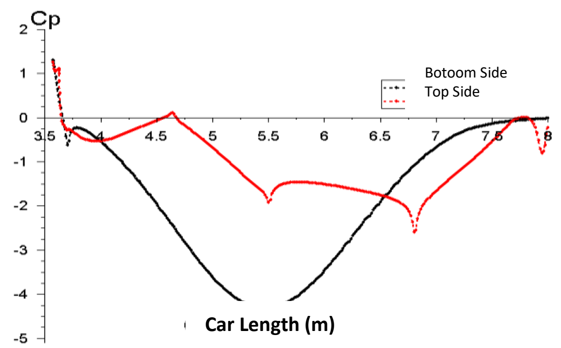

Fig 7: Pressure coefficient distribution on car when $\alpha = 20^0$

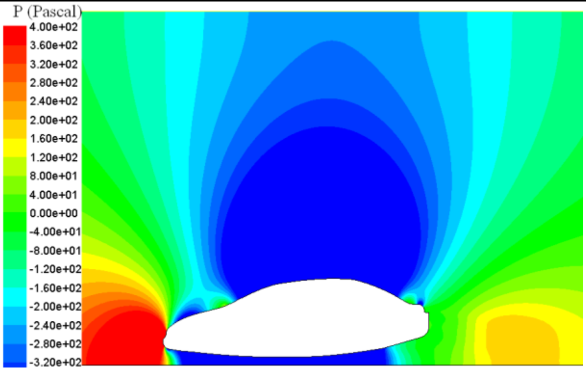

Fig 8: Pressure distribution on the calculation domain when $\alpha = 22^0$

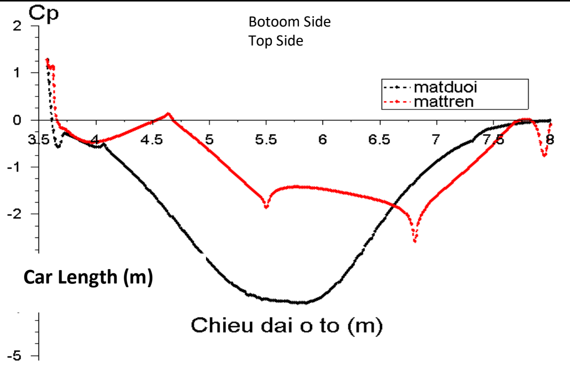

Fig 9: Pressure coefficient distribution on the car when $\alpha = 22^0$

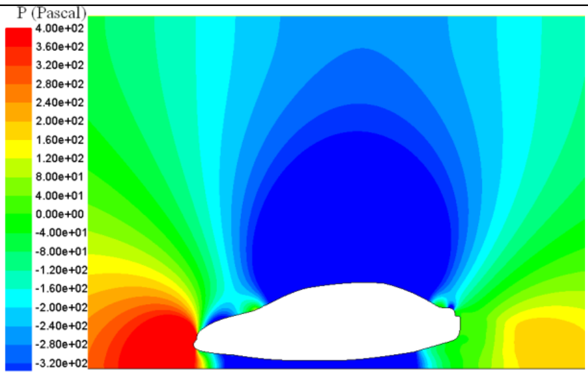

Fig 10: Pressure distribution on the calculation domain when $\alpha = 25^0$

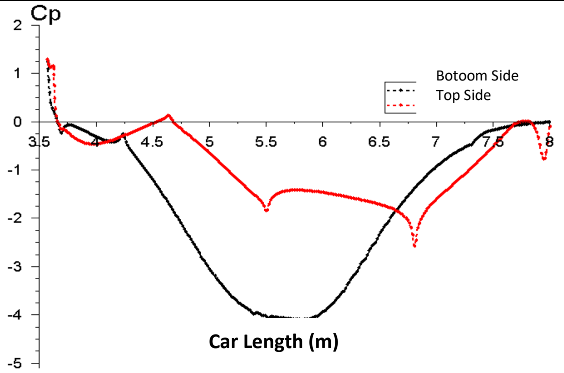

Fig 11: Pressure coefficient distribution on car when $\alpha = 25^0$

The results of the calculation of the drag and lift values that vary with α are shown in **Table 4.**

Table 4: Drag and lift values depending on the forward maneuvering angle α

α (degree)	**18**	**20**	**22**	**25**
C_d	0,345	0,304	0,29	0,258
D (N)	666,497	587,290	560,244	498,424
C_L	-5,11	-4,07	-3,97	-3,89
L (N)	987,1886	786,2735	766,9548	751,4998

Comment

In the above section, the simulation of the change in the drag coefficient C_d when changing the front maneuver angle α of the car is shown. When increasing the front maneuver angle, the pressure distribution on the underside of the car increases, so the car always tends to be lifted, causing the car's grip to decrease. The pressure above the car does not seem to change much. Therefore, in car design, the existence of an air flow below is undesirable. Under the car, there are many parts such as the engine, drive shaft, gearbox and some other parts exposed under the floor of the car. These parts block the air flow, causing turbulence as well as vortexing of the air flow below the floor of the car. Slow-moving air flows are the cause of increased lift according to Bernoulli's principle. In racing cars, people pay little attention to the maneuverability factor, to reduce aerodynamic drag, the front maneuver angle is significantly reduced. (Pham M.V., Plourde F. and Doan Kim S., 2003) [8, 9, 105].

3.2. Effect of rear maneuver angle β

In this section we consider the effect of aerodynamic forces acting on the car when the rear maneuver angle changes, the front maneuver angle $\alpha = 24^0$.

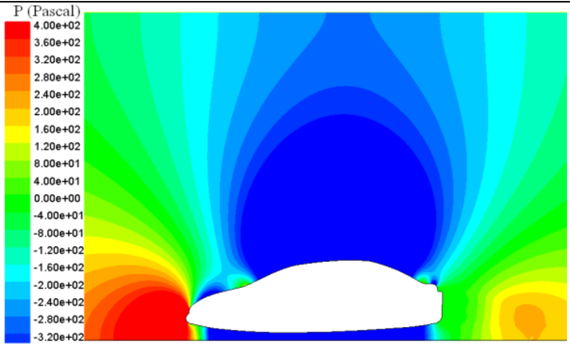

Fig 12: *Pressure distribution on the calculation domain when* $\beta = 16^0$

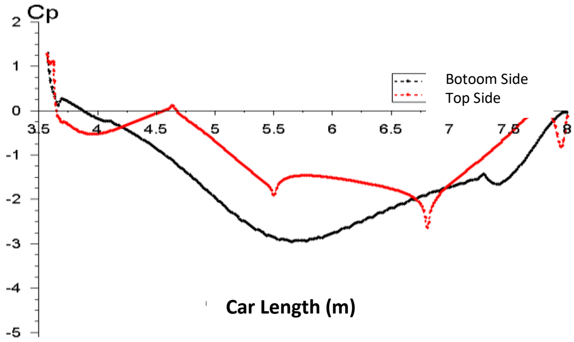

Fig 13: *Pressure coefficient distribution on car when* $\beta = 16^0$

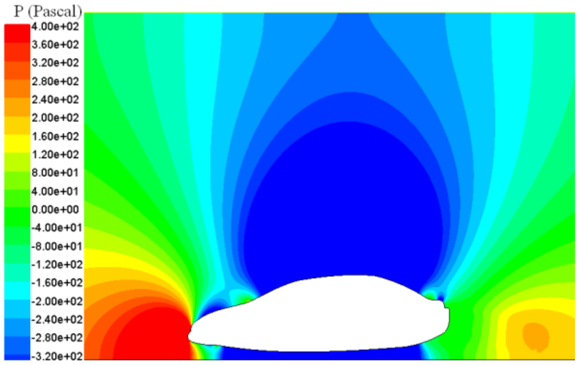

Fig 14: *Pressure distribution on the calculation domain when* $\beta = 18^0$

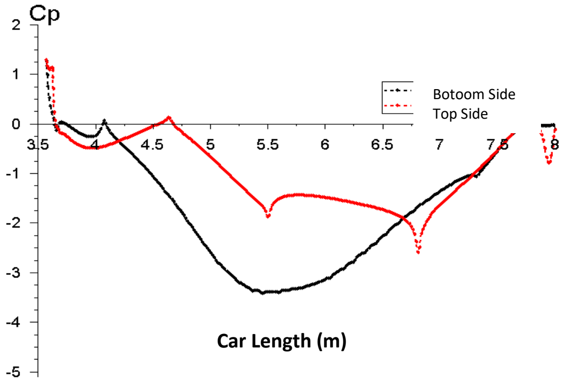

Fig 15: *Pressure coefficient distribution on car when* $\beta = 18^0$

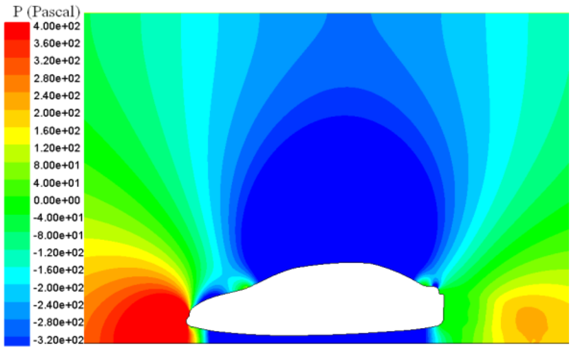

Fig 16: *Pressure distribution on the calculation domain when* $\beta = 20^0$

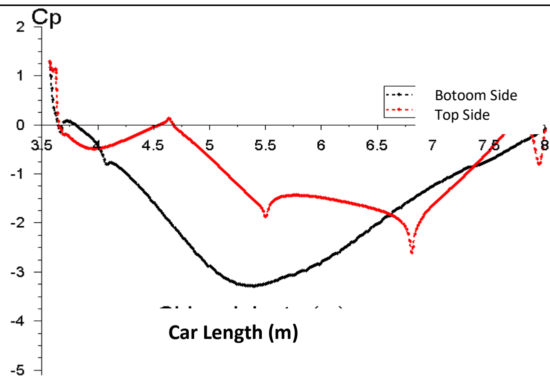

Fig 17: *Pressure coefficient distribution on car when* $\beta = 20^0$

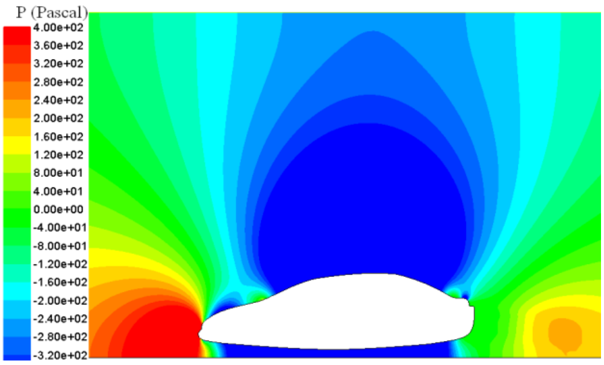

Fig 18: *Pressure distribution on the calculation domain when* $\beta = 22^0$

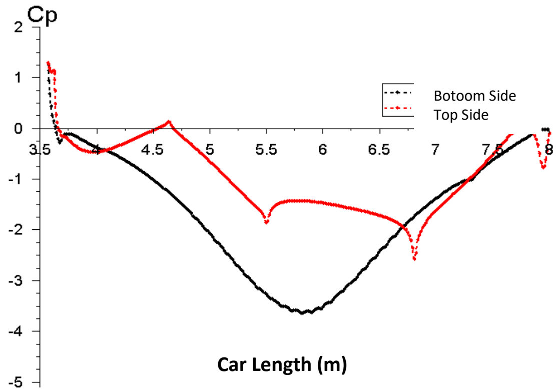

Fig 19: *Pressure coefficient distribution on the car when* $\beta = 22^0$

The results of the calculation of the drag and lift values that vary with β are shown in **Table 5**

Table 5: Drag and lift values depending on the rear maneuvering angle β

β (degree)	16	18	20	22
C_d	0,265	0,263	0,262	0,262
D (N)	511,947	508,083	506,151	506,151
C_L	-3,35	-3,29	-2,67	-2,65
L (N)	647,1785	635,5872	516,3904	511,9471

4. Comment

Based on the simulation results, in the case of the rear maneuver angle increasing, the pressure on the underside of the car decreases (shown on the pressure distribution graph). This is very similar to the outside reality, when the rear maneuver angle is large, the air flow under the car floor quickly escapes to the rear, which will reduce the vortex phenomenon under the car floor, thus also reducing the lifting force acting on the car. Therefore, for cars with high mobility (large front maneuver angle), in order to reduce the air resistance acting on the car, the rear maneuver angle is also designed to be as large as the front maneuver angle. (Pham M.V., Plourde F. and Doan Kim S., 2003) [11, 12, 17].

The pressure distribution on the top of the car also does not change much when changing the rear maneuver angle, so the force pressing the car down does not change much, so when designing the rear maneuver angle of the car, it is necessary to pay attention to the lifting force of the car, so that the value of this force is within the allowable limit, when the car is running at high speed, the car will not overturn. (Lamballais E., Sylvestrini S.H., 2002) [13, 142, 18].

5. Conclusion

The simulation calculation using Fluent software as a virtual laboratory achieved the following results:

The rear maneuvering angle of the car is from 22^0 to 25^0, the corresponding drag coefficient $C_d = 0.26$, will reduce the vortex of the air flow under the car floor, reducing the lift coefficient.

Research on the influence of crosswind force on the car.

The simulation calculation results are a source of documents for car designers to come up with some solutions in arranging and adjusting car parts.

Choosing the optimal speed for each specific car profile.

Compare the simulation results using the k - ε turbulence model with other models and Fluent software with other software to be able to come up with the most optimal solution method.

6. References

1. Piomeli U. High Reynolds number calculations using the dynamic subgrid-scale stress model. Physics of Fluids. 1993;A5:1484.
2. Smagorinsky J. General circulation experiments with the primitive equations. Monthly Weather Review. 1963;91(3):99-164.
3. Lyn DA, Rodi W. The flapping shear layer formed by flow separation from the forward corner of square cylinder. Journal of Fluid Mechanics. 1994;267:353-376.
4. Lyn DA, Einav S, Rodi W. A laser-Doppler velocimetry study of ensemble averaged characteristics of turbulent near wake of a square cylinder. Journal of Fluid Mechanics. 1995;304:285-319.
5. Durao DF, Heitor MV, Pereira JCF. Measurement of turbulent and periodic flows around a square cross-section cylinder. Experiments in Fluids. 1988;6:298-304.
6. Najm HN, Wyckoff PS, Knio OM. A semi-implicit numerical scheme for reacting flow. Journal of Computational Physics. 1998;143:381-402.
7. Pham MV, Plourde F, Doan Kim S. LES simulation in a thin liquid film submitted to high thermal stress. ASME Summer Heat Transfer Conference, Las Vegas (NV), USA, July 21-23, 2003.
8. Franke R, Rodi W. Calculation of vortex shedding past a square cylinder with various turbulence models. Proceedings of the 8th Symposium on Turbulent Shear Flows. 1991;189.
9. Lamder BE, Kato M. Modelling flow induced oscillations in turbulent flow around square cylinder. Proceedings of the Forum on Unsteady Flow (FED). 1993;157:189.
10. Lamballais E, Sylvestrini SH. Direct numerical simulation of interactions between a mixing layer and wake around a cylinder. Journal of Turbulence. 2002;3:28.
11. Khoa BQ. Researching, designing and manufacturing of the pollen bee vacuum dryer model. Ho Chi Minh City University of Technology; 2010.
12. Khoa BQ. Vietnam's renewable energy industry's approach to market development Impact of Smart grid systems and renewable energy sources integration. International Journal of Multidisciplinary Research and Growth Evaluation. 2024. DOI: https://doi.org/10.54660/.IJMRGE.2024.5.6.857-872.
13. Ngoc TM, Khoa BQ. Simulate Energy in Buildings According to LEED & LOTUS. Certification Science & Technology Publisher. 2023.
14. Ngoc TM, Khoa BQ. LEED Rating System Basis for Green Buildings. Certification Science & Technology Publisher. 2022.
15. Khoa BQ, Hay N, Duc LA, Tam PH. Optimization of The Vacuum Drying process for Bee Pollen Using the R method. International Journal of Multidisciplinary Comprehensive Research. 2024. DOI: https://doi.org/10.54660/IJMCR.2024.3.6.51-56.

16. Cong NC, Vuong PM, Nghia LTM, Khoa BQ. CFD Simulation of Convective air flow through a Square Cylinder. International Journal of Multidisciplinary Comprehensive Research. 2024. DOI: https://doi.org/10.54660/IJMCR.2024.3.6.57-62.
17. Cong NC, Vuong PM, Nghia LTM, Khoa BQ. CFD Simulation of Air Flow through Square Column. International Journal of Social Science Exceptional Research. 2024. DOI: https://doi.org/10.54660/.IJMRGE.2024.5.6.955-966.
18. Khoa BQ. Simulation Optimization of Vacuum Drying Process for Bee Pollen Using R Software. International Journal of Social Science Exceptional Research. 2024. DOI: https://doi.org/10.54660/.IJMRGE.2024.5.6.978-1013.